Shock Waves (2003) 13: 261–270
Digital Object Identifier (DOI) 10.1007/s00193-003-0215-0

Shock Waves

Design of a shock-free expansion tunnel nozzle in HYPULSE*

R.S.M. Chue, R.J. Bakos, C.-Y. Tsai, A. Betti

GASL Division, Allied Aerospace Industries, 77 Raynor Avenue, Ronkonkoma, NY 11779-6648, USA

Received 6 August 2002 / Revised version 18 July 2003 / Accepted 24 July 2003
Published online 21 October 2003 – © Springer-Verlag 2003
Communicated by F. Lu

Abstract. A shock-free expansion tunnel nozzle has been designed for the NASA HYPULSE facility at GASL. The main purpose of the nozzle is to increase the available test core size to accommodate a large-scale model, with the initial design intended for aeroheating studies at re-entry flow conditions. The nozzle was designed to expand the hypervelocity flow at the acceleration tube exit to a larger test core size of 30 cm, while maintaining a unit Reynolds number of at least 9.8×10^5/m. The two main challenges encountered in the design were the high entrance Mach number and the thick incoming tube-wall boundary layer. The paper discusses the design strategies of using a contour obtained using the method-of-characteristics as opposed to the conical geometry, and the skimmer versus the full-capture approaches, to achieve shock-free uniform exit flow with acceptable Reynolds numbers. To fully characterize the final design, computational fluid dynamics analyses were carried out using the nonuniform viscous flow profile at the acceleration tube exit as a start-line condition. The pitot pressure distribution at nozzle exit, as well as the heat flux on a hemisphere placed at nozzle exit, were calculated and compared with experiments. Besides discussing the fluid dynamic aspects of the design, a short description of a cost-effective manufacturing technique of fabricating the nozzle from fiberglass is also included.

Key words: Expansion tunnel, High enthalpy, Hypersonic nozzle, Nozzle design, Ground testing

1 Introduction

Shock-expansion tubes currently offer the only ground-test option for simulating near orbital speeds without the deleterious effects of driver gas contamination and/or facility erosion which plague more conventional reflected shock tunnels and arc-heated tunnels at hypervelocity conditions. Using a constant area acceleration tube to expand the flow to hypersonic conditions, the test flow in an expansion tube is delivered without the need for a conventional converging/diverging nozzle. However, the width of the useful test flow is limited by the diameter of the acceleration tube – currently 15.24 cm (6 in.) in the NASA HYPULSE Facility at GASL, the largest such facility in the U.S.

To access the full potential of the HYPULSE facility for aerothermal and aeropropulsion testing at hypervelocity conditions, a nozzle has been designed to be attached to the end of the acceleration tube to expand the 15.24 cm (6 in.) diameter, nominally Mach 7.5 acceleration tube exit flow to 60.96 cm (24 in.) diameter. The initial application of the nozzle was intended for aeroheating studies under re-entry flow conditions, and the design must be able to accommodate a sufficiently large model size, for data fidelity, and unit Reynolds numbers for the simulation of viscous and heating phenomena. Design constraints for this nozzle required a test flow core region of 30.48 cm (12 in.) in diameter while maintaining the nozzle-exit unit Reynolds number at or above 9.8×10^5/m (3×10^5/ft). Other nozzle entrance conditions were a pressure of 1 atmosphere at a total enthalpy of 21 MJ/kg (9000 BTU/lbm), or approximately 6 km/s velocity. The nozzle length was constrained to be within 2.54 m (100 in.) and was limited by the need for it to fit within the existing test section while leaving sufficient room for a test model. It was also desirable to keep the nozzle as short as possible so that the useful test time of the facility, approximately 0.5 ms, is not significantly reduced by the nozzle flow establishment process, and because hypersonic boundary layers can become quite large in long nozzles, effectively eliminating the useful test core.

A major difference between a classical convergent-divergent nozzle and an expansion tunnel nozzle is that the latter does not have a throat, but has a purely divergent section. Furthermore, the flow entering an expansion tunnel nozzle is already hypersonic, as opposed to the subsonic or low supersonic conditions found in nozzles with a choked throat. Thus, the nozzle must be designed to receive an already hypersonic flow and expand it further.

* An abridged version of this paper was presented at the 23rd International Symposium on Shock Waves at Fort Worth, Texas, July 23 to 27, 2001

Correspondence to: R.S.M. Chue
(e-mail: RChue@gasl-usa.com)

There are several key difficulties in the design of expansion tunnel nozzles. First, because the flow at nozzle inlet is already at a high Mach number, the nozzle is susceptible to shock generation. Shocks can be generated at the leading edge of the nozzle if the inlet has a smaller diameter than that of the acceleration tube, as in a skimmer nozzle, thus exposing the "lip" to the hypersonic incoming flow. Shocks and compression waves can also be produced at the wall contour, a problem that can be particularly severe in supersonic axisymmetric (as opposed to 2-D) nozzles (Migdal and Landis 1962; Darwell and Badham 1963; Migdal and Kosson 1965). The second difficulty is the strong boundary layer effects associated with the hypersonic nature of the facility. Not only can the wall boundary layers grow rapidly because of the high Mach numbers encountered throughout the nozzle, but the boundary layers delivered by the acceleration tube are also often very thick, a problem typical of expansion-tube facilities, so that the nozzle inflow profile is highly nonuniform, thereby making it more difficult to design for a uniform flow at the exit. Another problem in the design is the constraint of achievable unit Reynolds number, which requires the nozzle to have as large a mass capture (i.e., as small an area ratio) as possible. The design of shock-free and well-performing expansion tunnel nozzles can therefore pose serious challenges.

There have been two approaches in designing expansion tunnel nozzles – the "skimmer" and "full-capture" nozzles, each focusing on one of the difficulties discussed above. The skimmer or scoop-type nozzle has an inlet diameter that is smaller than the acceleration tube exit such that the tube wall boundary layer is bled and a more uniform flow profile is passed to the nozzle. The skimmed inlet flow could thus allow a fresh boundary layer to start at the inlet lip and may also take advantage of the delayed laminar-to-turbulent transition at high Mach numbers, both of which could lead to a decreased inflow boundary layer thickness. On the other hand, the smaller entrance diameter has the disadvantage of having a larger nozzle area ratio for the same required nozzle-exit core diameter, and thus implies a reduced unit Reynolds number at the exit. A further disadvantage is the need to accommodate the shock system formed at the skimmer leading edge. The skimmer design was used for the first nozzle built for a large expansion tunnel as carried out by NASA on the Langley 6-inch expansion tube (Miller 1976), the original name for the HYPULSE facility when it was first built at the Langley Research Center in the late 1960's. The skimmer nozzle designed by Miller (1976) was a 10° conical nozzle with a 8.89 cm (3.5 in.) inlet from a 15.24 cm (6 in.) acceleration tube expanding to 63.5 cm (25 in.) exit diameter. The alternative of a full-capture design was previously tried by GASL (also in HYPULSE) for a 4:1 area ratio contoured nozzle built for aeropropulsion testing (Bakos et al. 1996a). The nozzle was only required to expand from Mach 4.77 to 6.4 with a 30.48 cm (12 in.) exit diameter, and therefore the flow requirement was more modest when compared to the current specifications.

The two previous designs also illustrated another issue in hypersonic nozzle design strategy – the contoured versus conical geometry. While contouring of the wall profile could lead to uniform exit flow, it is more susceptible to flow nonuniformities at off-design operating conditions due to the focusing nature of the contoured profile. Conical nozzles are simpler to design and are less sensitive to off-design conditions, but one has to be content with the slightly diverging and expanding flow at the nozzle exit. As a whole, neither of the two previous designs appear to be completely satisfactory. For Miller's (1976) skimmer nozzle, the achieved unit Reynolds number was only 1.6×10^4/m and an annular shock in the exit flow was also evident, illustrating the nonuniform nature of the nozzle flow. For the full-capture nozzle (Bakos et al. 1996a), uniform flow was also not achieved, even though the nozzle wall contour was designed to produce fully uniform flow.

In this study, the issues of skimmer versus full capture and contoured versus conical design strategies have been revisited in order to achieve a compact design to satisfy the current requirements of increasing test core size while maintaining the unit Reynolds number. The skimmer nozzle was first attempted, but the full-capture nozzle was also studied. The need to accommodate the rather thick tube-wall boundary layer that is characteristic of high pressure expansion tube operation (Bakos et al. 1996b) complicates the nozzle design and trades against the larger capture area of the nozzle for producing a large core flow size. The paper addresses the issues that led to the final design selection. Installation and calibration of the nozzle have been carried out for enthalpies of 22.6 and 11.5 MJ/kg, showing a capability of hypervelocity testing of models up to 30.48 cm (12 in.) wide.

2 Computational methods

In this work, the design and analyses were carried out using the method-of-characteristics and computational fluid dynamics (CFD). CFD was performed using the GASP version 3 code (McGrory et al., 1996). In preliminary design analyses, the gas was assumed to be perfect with a constant ratio of specific heats γ. In the final verification of the design with experiments, the gas medium was multi-species chemically reacting air, where the NASP finite-rate chemistry model was used and the thermodynamic properties were provided by the NASA Lewis equilibrium curve fits with 10 coefficients. The boundary layers are assumed to be turbulent throughout the nozzle. At the acceleration tube exit (i.e., nozzle inlet), the flow is fully turbulent in the tube with a unit Reynolds number of 2×10^7/m at the design condition of 21 MJ/kg. Thus, the turbulent assumption is quite valid for full capture nozzles. For skimmer-type nozzles, the boundary layer will restart at the nozzle tip, provided that the tube boundary layer is completely bled off. However, the laminar-to-turbulent transition distance for the current tube-exit unit Reynolds number is relatively short (Adam 1997) and would oc-

cupy only a small percentage of the total nozzle length. As a result, the turbulent boundary layer assumption is also adopted when designing and analyzing skimmer nozzles for the current conditions considered. The Baldwin–Lomax algebraic turbulence model is used to describe the wall boundary layers.

3 Preliminary nozzle profile – skimmer nozzles

As noted in the Introduction, the flow at the acceleration tube exit is quite nonuniform due to the development of thick wall boundary layers. The design of the nozzle was thus carried out in two stages – the preliminary design considered the simplified case of uniform flow at the nozzle inlet, while the final design incorporated the effect of inlet flow nonuniformity. Since the skimmer nozzle may be able to avoid ingesting the boundary layers, it was considered first. The study focused on a skimmer-type inlet having a diameter of 10.16 cm (the diameter of the expansion tube being 15.24 cm).

The preliminary design of the nozzle wall profile examined three possible configurations: 1) a fully contoured profile that would deliver uniform exit flow, 2) a simple conical nozzle that would have acceptable flow divergence and reasonable flow uniformity, and 3) a contoured inlet followed by a conical profile to reduce nonuniformities, while keeping the design simple.

3.1 Contoured nozzle

The contoured skimmer nozzle was designed using the method-of-characteristics to receive uniform inflow and to yield fully uniform Mach number and pressure at the nozzle exit. The resulting contour consists of an outward turning expansion section followed by a wave cancellation section of opposite curvature. Viscous effects could be accounted for by correcting the wall profile with the displacement thickness along the wall.

The design is performed by assuming the nozzle to expand from an inlet Mach number of 7.5 to an exit Mach number of 16. The inviscid method-of-characteristic procedure (before viscous correction) resulted in a nozzle length of approximately 8.08 m and an exit diameter of approximately 81.28 cm. The nozzle obtained far exceeds the imposed length limitations of 2.54 m. To examine the flow quality and to evaluate the validity of the design, an inviscid CFD calculation was carried out for the nozzle contour. Shown in Fig. 1 is the Mach number distribution in the front portion of the nozzle. The designed inlet lip has a finite expanding wall angle and expansion waves can be observed to originate from there. However, compression waves or shocks of significant magnitude were found in the nozzle, destroying the flow uniformity. These pressure waves appear to originate from around the junction between the expansion and wave-cancellation sections of the wall contour, where the second derivative of the wall profile becomes negative.

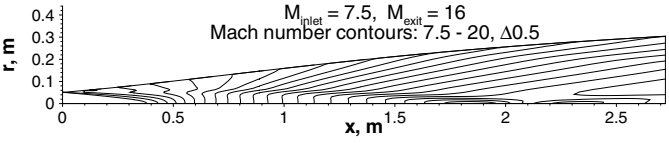

Fig. 1. Inviscid CFD solution of contoured skimmer nozzle designed using the method of characteristics. Only the front portion of the nozzle is shown

The existence of compression waves is unique to axisymmetric (as opposed to 2-D) nozzles and has been identified as a consequence of flow turning during the expansion phase of the nozzle. For axisymmetric nozzles, the flow is found to turn to an angle larger than that of the wall. After the expansion phase, the flow must be turned back to satisfy the wall boundary condition, which then leads to the generation of the compression waves (Migdal and Landis 1962; Darwell and Badham 1963; Migdal and Kosson 1965; Callis 1966).

There are two possible reasons for the failure of the design method to eliminate the compression waves: 1) the current method-of-characteristics code used did not produce a sufficiently smooth wall profile and pressure waves were generated as the wall curvature turns negative, 2) the compression waves are especially severe for the hypersonic inlet condition the present nozzle is operating at and, therefore, pressure waves due to wall perturbations could be more drastically amplified than those encountered in transonic inlets in classical nozzle designs. More recently, a nozzle contour designed using the method-of-characteristics code of Jacobs (2000) was able to decrease the magnitude of the compression waves, indicating that the cause of failure may be due to the first reason. However, the improvement was only observed when the inflow is uniform. When the inflow is highly nonuniform, the designed nozzle was unable to deliver uniform outflow.

Indeed, for the current tunnel operating conditions, the flow at the expansion tube exit is expected to suffer from thick boundary layers, which would generate a highly nonuniform flow at the nozzle inlet and a significant amount of viscous layer at the exit that occupies approximately half of the exit radius. It is therefore questionable that the conventional method-of-characteristics-plus-displacement-thickness design method could achieve uniform exit flow. A different design approach was thus sought to overcome this difficulty.

3.2 Conical nozzle

Considering the difficulty with the contoured nozzle design, strictly conical geometries were considered next. A 10° nozzle had been used previously by Miller with some success (Miller 1976), although for a lower enthalpy and unit Reynolds number.

Simple conical skimmer nozzles with half divergence angle of 5.71°, 8°, and 10° have been examined for the current design condition. All three nozzles have inlet diameters of 10.16 cm and exit diameters of 60.96 cm, where the exit diameter is selected with the expectation that

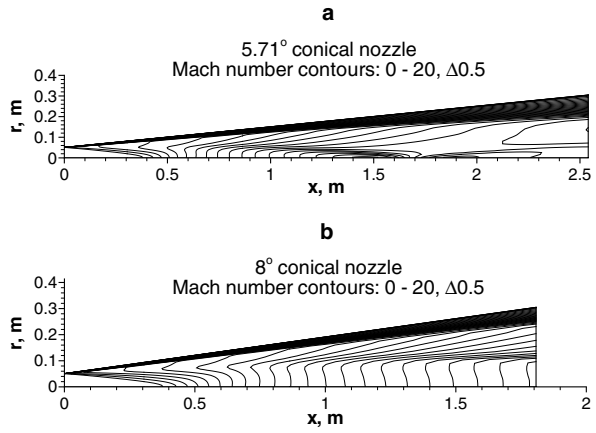

Fig. 2a,b. CFD solution for the conical skimmer nozzles, fully turbulent with uniform inflow: **a** 5.71°, **b** 8°

the required core flow would occupy half the exit dimension. For the 5.71° nozzle, the divergence angle is directly given by the maximum allowable length (2.54 m). The 10° nozzle is expected to produce the largest acceptable flow divergence, while maintaining the shortest length.

Full viscous CFD computations were performed for the three conical skimmer nozzles with uniform inlet flow. The boundary layers in the nozzles are assumed turbulent. The solutions for the 5.71° and 8° nozzles (Fig. 2) show that a leading-edge shock occurs at the inlet lip and it propagates toward the centreline, destroying the flow uniformity as it did in the contoured nozzle.

For the 10° nozzle, a compression wave is also observed to originate from the inlet lip, but the angle of propagation is such that the wave diverges from the centreline, leaving a 15 cm radius uniform core at the nozzle exit. The computational result for the 10° nozzle is plotted in Fig. 3 where the compression wave can be seen in the Mach number contours. The density distribution, which closely resembles the shape of the pitot pressure distribution, shows the existence of uniform core flow, not unlike that found in the conical nozzle of Miller (1976). The above results illustrate that the wall angle in the conical design must be sufficiently large in order for the leading edge shock to diverge from the nozzle core. The 10° nozzle would therefore be the only suitable configuration among the three conical designs. The unit Reynolds number at nozzle exit for the 10° case is 1.3×10^6/m.

The performance of the conical design under the influence of nonuniform inlet flow was examined next. Experimental data from the HYPULSE acceleration tube exit plane showed that flow nonuniformity due to the wall boundary layer extends into the central 10.16 cm diameter (skimmer inlet), and thus its effect must also be included in the design. Viscous CFD computations with nonuniform inlet flow was therefore performed for the simple 10° conical nozzle.

The nonuniform inlet flow condition for the nozzle is computed by assuming that the axial velocity at the expansion tube exit follows a 1/7th power law based on the tube area and that the boundary layer occupies the full cross section – the boundary layer edge occurs at the centreline – while static pressure remains uniform. This condition was expected to be the worst case and was adopted for the design analysis. The numerical results (Fig. 4) revealed that the nonuniform inlet flow caused the inlet compression wave to diverge at a lower angle, reducing the uniform core radius from the required 15.24 cm to about 11 cm. The effect of the nonuniform inlet flow is equivalent to a drastic increase in the boundary layer due to the inheritance of the already-developed boundary layer from the acceleration tube. The much larger displacement effect results in an effective nozzle wall curvature that continuously decreases in slope ($d^2r/dx^2 < 0$), which then causes the inlet compression wave to converge towards the centreline and reduces the core size. The simple conical nozzle is therefore incapable of accommodating the highly nonuniform inflow encountered in the current operating condition.

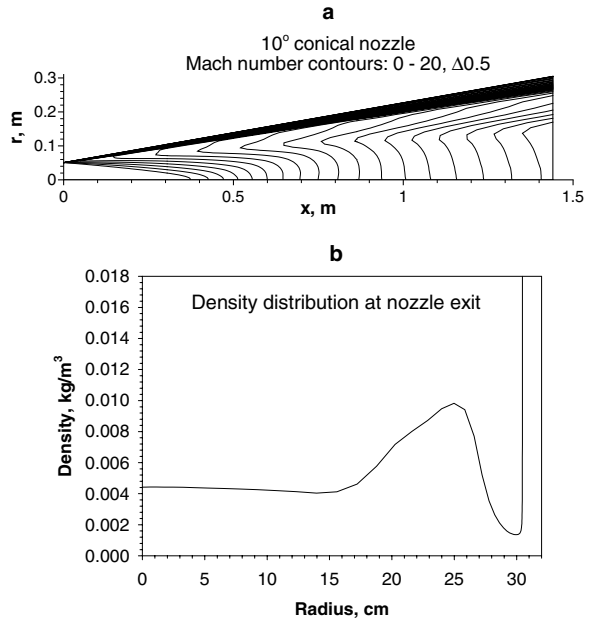

Fig. 3a,b. CFD solution for 10° conical skimmer nozzle, fully viscous solution with uniform inflow. **a** Mach number contours. **b** Density distribution at nozzle exit

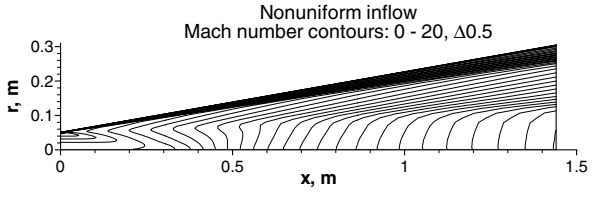

Fig. 4. Mach number distribution for 10° conical skimmer nozzle, fully viscous solution with nonuniform inflow

4 Contoured inlet asymptoting to a conical profile

It is apparent from the above design analyses that the occurrence of compression waves or leading edge shock is the major cause of flow nonuniformity at the nozzle exit.

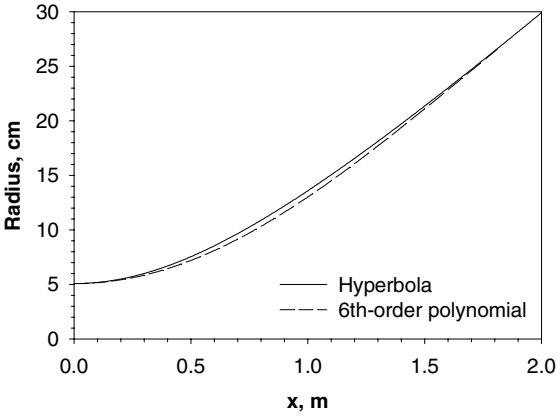

Fig. 5. Two possible nozzle profiles with continuously expanding sections

To eliminate or reduce the magnitude of the compression wave, the literature has suggested using a gradually turning nozzle inlet, following by a wall section as determined by the method-of-characteristics to produce a region of uniform Mach number at the centreline before connecting to a conical section (Migdal and Landis 1962; Darwell and Badham 1963; Migdal and Kosson 1965; Callis 1966). This procedure is indeed no different from the method-of-characteristics design procedure as described earlier for the contoured nozzle design, except for the final conical profile. However, as discussed earlier, this procedure is unsatisfactory for the current design requirements.

The results of the contoured nozzle point toward the possibility of eliminating the occurrence of the compression wave by having a nozzle contour with a continuously expanding section (i.e., the second derivative of the wall profile remains positive throughout the nozzle). The conical nozzle solutions discussed above also indicate that, to accommodate thick boundary layers, the slope of the conical profile must increase, otherwise the displacement effect would generate compression waves which would then converge towards the centreline and affect the core flow. A strategy was therefore formulated to design a shock-free nozzle and to improve exit flow uniformity by having an expansion section that asymptotically approaches a conical contour, with the inflexion point located either at or downstream of the nozzle exit.

Two possible mathematical representations that would yield such a contour are the hyperbola and the 6th-order polynomial. Inviscid CFD calculations have been carried out for 1) a hyperbolic profile and 2) a 6th-order polynomial profile, that have continously expanding sections along the nozzle lengths. For both profiles, the nozzle inlet diameter is 10.16 cm (4 in.) and the exit diameter is 60.96 cm (24 in.) For the hyperbola, the nozzle length is set at 2.032 m (80 in.), resulting in the following equation which is nondimensionalized with the inlet radius:

$$\frac{(r-r_0)^2}{b^2} - \frac{x^2}{a^2} = 1,$$
$$r_0 = 1, \quad a = 18.013, \quad b = 3.483. \tag{1}$$

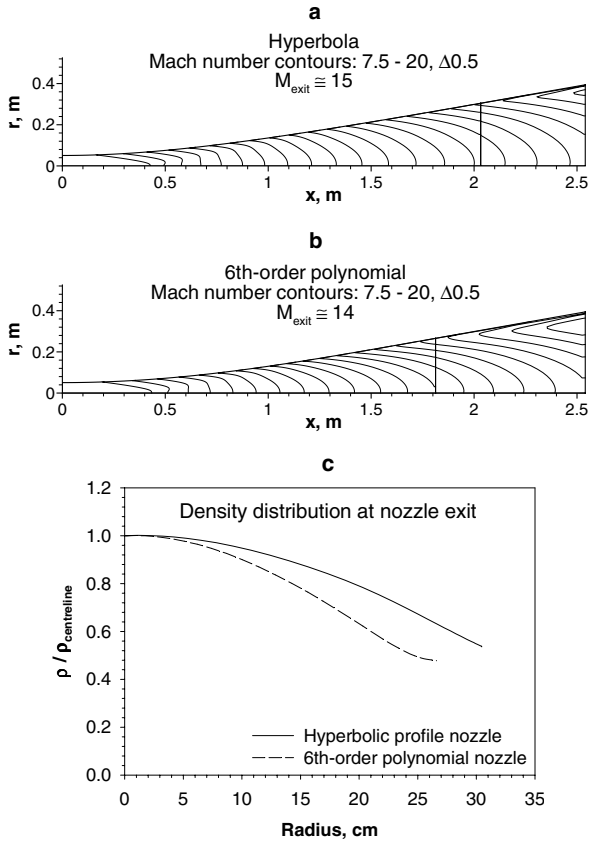

Fig. 6a–c. Inviscid CFD solutions for skimmer nozzles with uniform inflow. Mach number contours for **a** hyperbolic profile and **b** 6th-order polynomial. **c** Comparison of normalized density distributions at nozzle exit

For the 6th-order polynomial, the nondimensionalized equation is:

$$r = ax^6 + cx^4 + ex^2 + f,$$
$$a = 1.445 \times 10^{-10}, \quad c = -1.038 \times 10^{-6},$$
$$e = 4.416 \times 10^{-3}, \quad f = 1. \tag{2}$$

resulting in an inflexion point (zero wall curvature) at an axial location of 1.813 m (71.37 in.), chosen to be the length of the nozzle. The two profiles are plotted in Fig. 5. The inviscid CFD results shown in Fig. 6 demonstrate the possibility of shock-free flows, with the hyperbola yielding a more uniform flow at nozzle exit. It appears that the better uniformity generated in the hyperbolic profile is due to its more rapid initial expansion (larger initial wall divergence) than the polynomial profile (see Fig. 5). This indicates that, to improve flow uniformity at nozzle exit, the flow expansion should preferably be accomplished near the inlet so that a conical flow is asymptotically approaching at the exit.

While these profiles are successful in eliminating the compression waves, small nonuniformities due to the expanding flow are observed in the centreline region at nozzle exit, although these nonuniformities are far lower than those caused by the leading-edge compression. For the hyperbolic profile, the variation in density (and similarly the

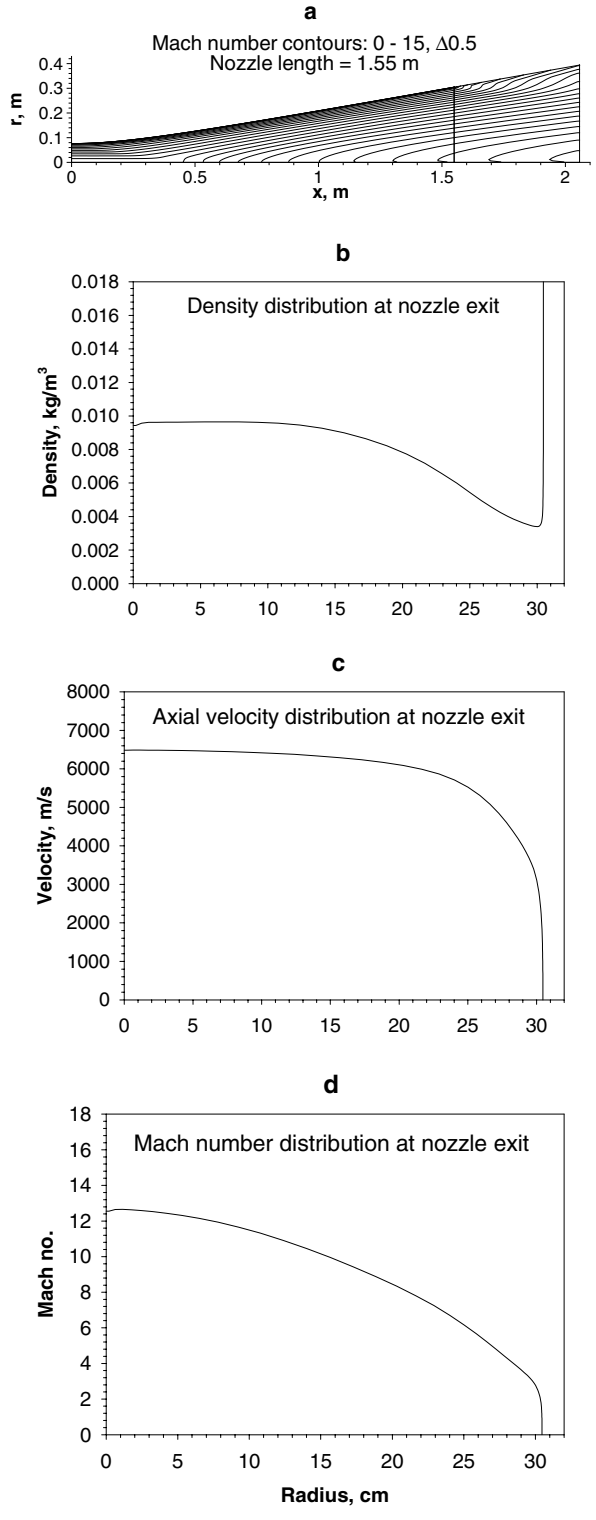

Fig. 7a–d. Fully turbulent CFD solution for the final designed full-capture hyperbolic nozzle with nonuniform inflow. **a** Mach number contours. **b** Density distribution at nozzle exit. **c** Axial velocity distribution at nozzle exit. **d** Mach number distribution at nozzle exit

dynamic pressure, since the axial velocity is quite uniform) between the centreline and at 15.24 cm (6 in.) radius at nozzle exit is approximately 15%. The unit Reynolds number at nozzle exit is 18.7×10^5/m (5.7×10^5/ft) and decreases to 13.12×10^5/m (4×10^5/ft) at 50.8 cm (20 in.) from the exit. Since the unit Reynolds number still exceeds the design target (of 9.8×10^5/m), it appeared possible that the nozzle profile could be fine tuned to reduce the centreline nonuniformity by varying the degree of expansion through either changing the nozzle length or divergence angle.

Several hyperbolic nozzle configurations were further investigated and the results indicated that the degree of uniformity at the nozzle exit would depend on both the level of inflow nonuniformity as well as the expansion rate and length of the nozzle. A design technique began to emerge which utilizes smooth but rapid initial expansion while limiting the flow divergence angle through the control of the inlet diameter, the nozzle length, and the final divergence angle. The design strategies devised to improve the flow uniformity of the nozzle can be summarized as follows:

1. The rate of geometric expansion should be most rapid near the inlet and decreases toward the exit, so that the generation of expansion waves is confined to the inlet region of the nozzle and a conical flow is approached at the exit. The hyperbola is preferred over the 6th-order polynomial and it also has the inflexion point at infinity.
2. The wall divergence angle at nozzle exit should be minimized to reduce the amount of flow divergence. On the other hand, the rate of geometric expansion throughout the nozzle is bounded by the wall divergence angle at the exit. Since the viscous layer growth along the nozzle will result in smaller effective local wall angles and may thus result in the generation of compression waves, a small exit divergence may affect the uniformity of the exit flow. Furthermore, the wall divergence should not be too small and result in an overly long nozzle, as the boundary layer can grow rapidly to reduce uniformity. An exit half-angle of 10° has been found to be a satisfactory compromise.
3. The length of the nozzle should be such that the expansion waves propagating from the inlet contour are furthest from the centreline at nozzle exit. If, however, the expansion waves cross the centreline at nozzle exit, flow uniformity there will be severely affected.

Because of the highly nonuniform nature of the inlet flow, the design was performed using CFD computations that incorporate fully viscous effects with inflow nonuniformity and by following the above strategies. Indeed, in the final design studies, it was found that a full-capture nozzle, having the same inlet diameter as the expansion tube, with a hyperbolic profile could be designed to deliver the required uniform exit-core diameter by tuning the length and expansion rate of the profile. Because of the larger inlet diameter, the area ratio of the full-capture nozzle is lower, and hence the Reynolds number at the nozzle exit is more favorable than for the skimmer design.

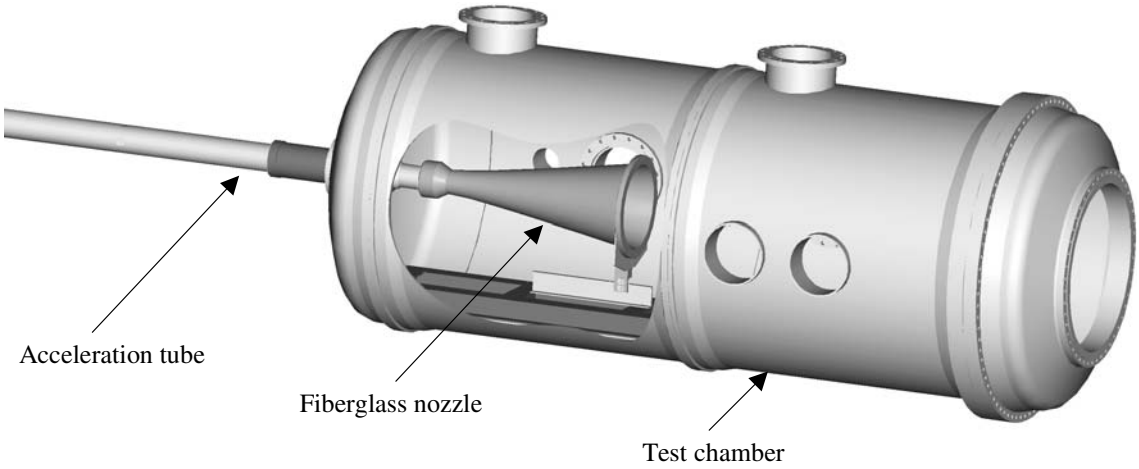

Fig. 8. Rendered design drawing of the hyperbolic, full-capture nozzle installed in HYPULSE

The final optimum design has a hyperbolic profile having a length of 1.5494 m, exit diameter of 60.96 cm, and maximum wall angle (at nozzle exit) of 10°. The equation for the hyperbola, nondimensionalized with the inlet radius, is:

$$\frac{(r-r_0)^2}{b^2} - \frac{x^2}{a^2} = 1,$$
$$r_0 = 1, \quad a = 4.04487, \quad b = 0.727195. \tag{3}$$

The resulting nozzle can be considered as a conical nozzle that has a smooth inlet expansion section with no inflexion point to avoid the generation of compression waves, while having a wall profile with a continuously increasing slope to accommodate the boundary layer growth.

Fully viscous CFD solutions for the uniform inlet case show that the resulting nozzle flow is indeed shock free with a uniform, though slightly diverging, core at nozzle exit. Even when the inlet nonuniformity is included, the nozzle remains shock free and with a sufficiently wide core. The fully turbulent solution with nonuniform inflow is shown in Fig. 7. From the figure, the density in the core is quite uniform with only a few percent difference between the centreline and at 15 cm radius. At high stagnation enthalpies, the pitot pressure, p_{t2}, can be approximated by:

$$p_{t2} \simeq 0.92\rho u^2 \tag{4}$$

where ρ is the density and u is the velocity. Since the axial velocity remains relatively uniform, as shown in Fig. 7, the pitot pressure is also quite uniform. The Mach number and static pressure (not shown) distributions at nozzle exit are less uniform than the density, due to the expanding nature of the flow. However, because the nozzle was primarily designed for experiments at re-entry level enthalpies, the main flow parameter of interest was dynamic (or pitot) pressure rather than Mach number and static pressure. Thus, the flow quality of the nozzle was mainly judged by the pitot pressure uniformity in the solution. The unit Reynolds numbers at nozzle exit and at 50.8 cm downstream are, respectively, 1.8×10^6/m and 1.2×10^6/m, which are within the required design target range.

5 Mechanical design and fabrication

The mechanical design for the nozzle was carried out at GASL. A cost effective technique of fabricating nozzles from fiberglass has been developed and was applied to the current expansion tunnel nozzle.

The manufacturing process begins with the construction of a polyurethane foam mandrel that is machined to the nozzle contour. A stainless steel insert that contains the initial portion of the nozzle contour is placed on the mandrel. This portion of the nozzle provides attachment points to the end of the expansion tube and eliminates upstream-facing sharp edges in the fiberglass. A release agent is placed on the mandrel to facilitate nozzle and mandrel separation. The fiberglass with a polyester resin is then wrapped on the mandrel to form the nozzle. An end flange is manufactured from the polyester resin and then attached to the nozzle exit during the wrapping process. After the resin has thoroughly cured, the nozzle is removed from the mandrel and a final polishing of the flow surface is performed. Due to the choice of a "zero shrink" resin, the resulting nozzles have been found to closely match to mandrel contour. A steel track and roller system was designed and attached to the nozzle end flange to provide support to the nozzle while allowing the nozzle to move relative to the test section during testing. The nozzle installed in the test section is shown in Fig. 8.

6 Verification with experiments

While the nozzle was designed for a re-entry level total enthalpy of 21 MJ/kg, calibrations for 23 and 12 MJ/kg were carried out. In order to accurately verify the design, CFD solutions for the two operating conditions were obtained and compared with experiments. The key results for the calibration conditions are giving below. Details of the experiments are provided in the references of Chue et al. (2002), Rogers et al. (2001), and Foelsche et al. (2001).

The nozzle inflow conditions were evaluated from experimental measurements that include static pressure, pi-

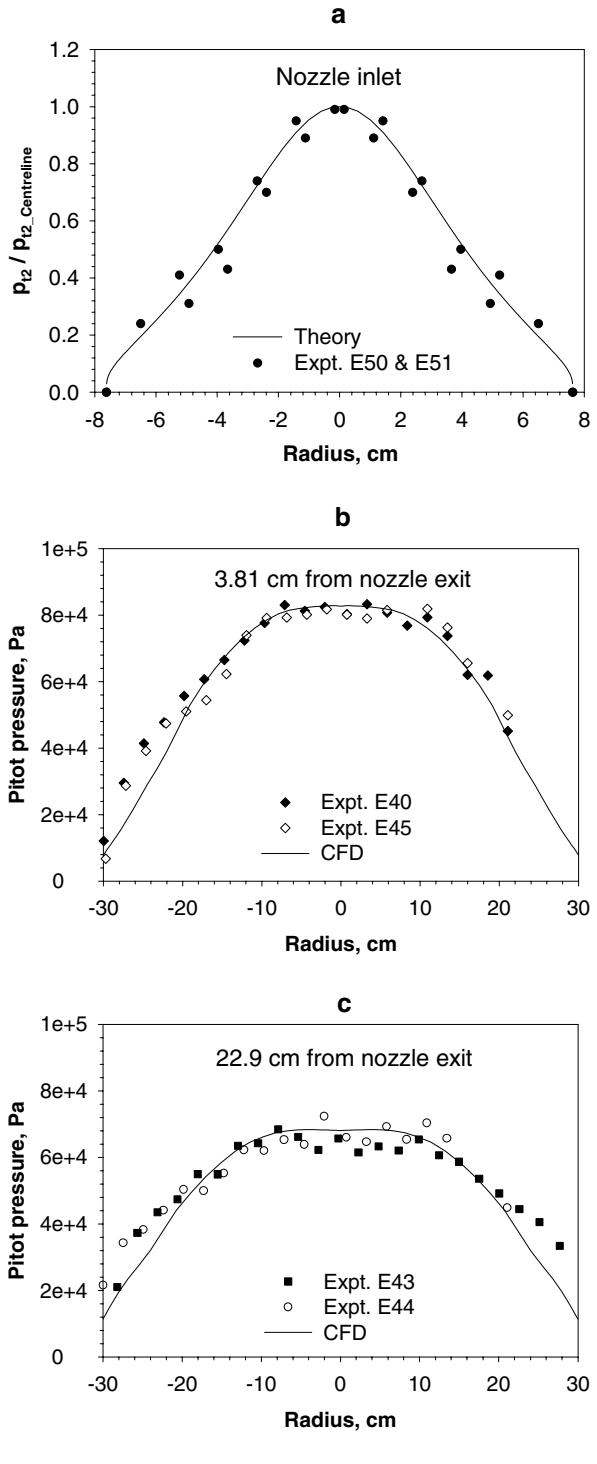

Fig. 9a–c. Verification of CFD solution with experimental nonuniform inflow close to design point. H_t = 22.6 MJ/kg, p_{inlet} = 20.6 kPa, T_{inlet} = 1627 K, M_{inlet} = 8.3. **a** Pitot pressure distribution at nozzle inlet. **b** Pitot pressure distribution at 3.81 cm from nozzle exit. **c** Pitot pressure distribution at 22.9 cm from nozzle exit

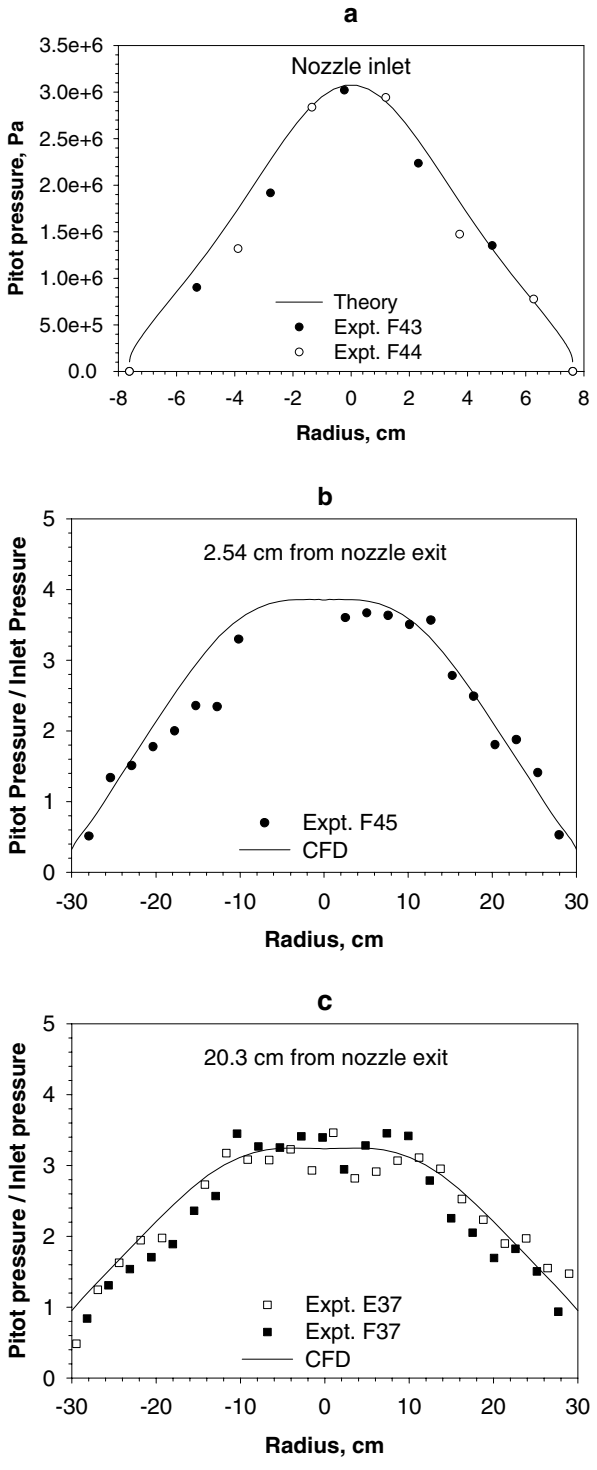

Fig. 10a–c. Verification of CFD solution with experimental nonuniform inflow condition at H_t = 11.5 MJ/kg, p_{inlet} = 41.5 kPa, T_{inlet} = 976 K, M_{inlet} = 7.6. **a** Pitot pressure distribution at nozzle inlet. **b** Pitot pressure distribution at 2.54 cm from nozzle exit. **c** Pitot pressure distribution at 20.3 cm from nozzle exit

tot pressure, and shock speeds. The measured pitot survey was found to be even more nonuniform than that assumed in the design. In the final CFD analyses, the inflow velocity profiles were assumed to follow a 1/5th power law (as opposed to the 1/7th law for the design analyses) and that the inflow was in chemical equilibrium. In the nozzle, the flow was assumed to be turbulent and finite-rate chemical kinetics were used. The pitot pressure profiles, computed by assuming chemical equilibrium, at the nozzle inlet and exit for 22.6 MJ/kg enthalpy are plotted in Fig. 9. The results illustrate the existence of a uniform core at the nozzle exit, which agrees with the experiments. Similar results for the lower enthalpy level of 11.5 MJ/kg are plotted in Fig. 10.

As a further characterization of the nozzle flow, the heat flux on a hemisphere placed downstream of the nozzle was also computed and compared with measurements. For this calculation, the upstream boundary condition to the sphere was obtained directly from the nozzle CFD solution. The boundary layer over the sphere was assumed laminar and the chemical kinetics model of Park (1993), which can accommodate high stagnation temperatures, was used. The hemisphere was made of a ceramic material (Macor) and coated with aluminium oxide (Al_2O_3). The wall surface was assumed to be noncatalytic at a temperature of 423 K in the computation. The viscosity and thermal conductivity were calculated using Sutherland's formulae, while the species diffusion was evaluated using a constant Schmidt number of 0.7. The predicted heat flux at the 22.6 MJ/kg enthalpy condition with a 1.905 cm diameter hemisphere is plotted in Fig. 11, showing agreement with experiments as well as with the stagnation point heat flux obtained using the Fay-Riddell theory.

The transient performance of the nozzle can be seen from the pressure time history in Fig. 12 taken from Chue et al. (2002). In the figure, the wall static pressure at the acceleration tube exit is plotted with the nozzle exit pitot pressure for experiment F30 at 22.1 MJ/kg. At tube exit, the sudden increase in static pressure signifies the arrival of the secondary shock and the acceleration gas. The test gas interface is estimated to arrive at approximately 0.1 ms after flow arrival and is indicated by the small increase in slope of the pressure trace. At nozzle exit, the pitot pressure exhibits a more complex starting process as larger pressure fluctuations can be seen when the flow arrives. The nozzle exit starting flow is characterized by a sharp increase in pressure followed by a decrease and then a relatively quasi-steady flow period, representing the events of the arrival of a complex starting shock system followed by the test gas interface. Although the nozzle starting process does take a finite amount of time to occur, flow unsteadiness appears to be mainly limited to the period during the passage of the acceleration gas, while leaving the test gas flow relatively unaffected. Indeed, Fig. 12 shows that the behavior of the nozzle inflow and outflow pressure traces appears to be similar so that the available test time is not penalized by the addition of the nozzle to the expansion tube. Previous experimental studies of expansion tunnel operations also support this observation, and in some

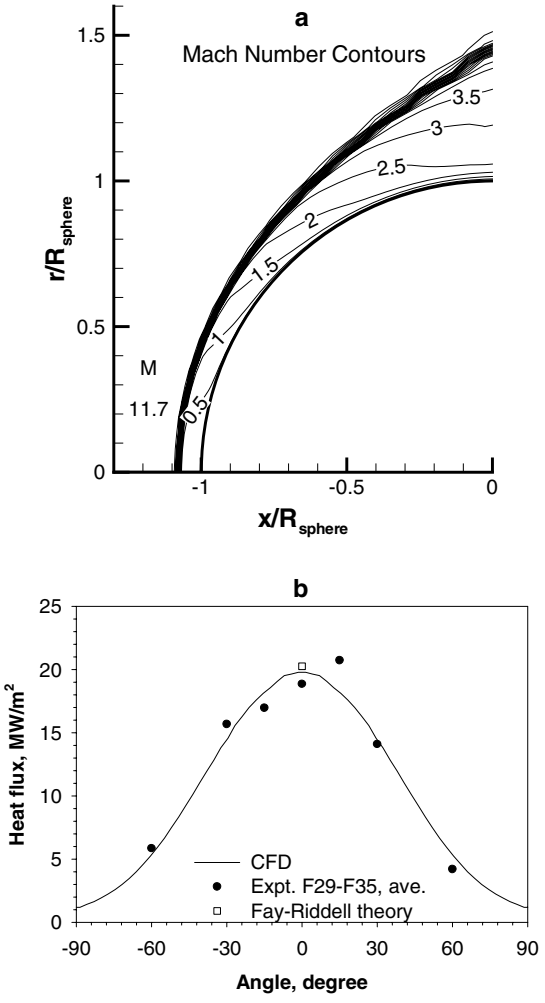

Fig. 11a,b. Heat flux calculation over a hemisphere at 22.6 MJ/kg (same condition as in Fig. 9). Hemisphere diameter = 1.905 cm, sphere "nose" located at x =13.3 cm, r =11.7 cm from nozzle exit. **a** Mach number contours. **b** Heat flux distribution. Experimental data and Fay-Riddell theoretical value taken from Chue et al. (2002)

cases (for small nozzle area ratios), the test time in expansion tunnel mode operation could even be slightly longer than in expansion tube mode (Miller 1976). For the two enthalpy levels studied, the test window is taken approximately between 0.2 to 0.55 ms after flow arrival.

For the experimental data shown, the pressure sensors have 500 kHz frequency response and sensitivities ranging from 1 to 100 mV/psi, with a measurement uncertainty of less than 5%. Heat flux gages are platinum thin-film resistance thermometers painted on machinable ceramic substrates and are manufactured and calibrated at GASL. The uncertainty in heat flux measurements are less than 20%. Further details of the operation of the facility, flow measurements, and data uncertainty can be found in the references of Chue et al. (2002), Rogers et al. (2001), and Foelsche et al. (2001).

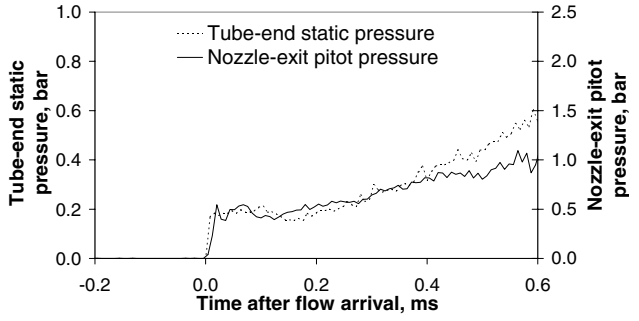

Fig. 12. Pressure time history at upstream and 2.54 cm downstream of nozzle. Taken from experiment F30 for H_t = 22.1 MJ/kg

7 Conclusions

An expansion tunnel nozzle has been designed to further enhance the hypervelocity testing capabilities of the HYPULSE Facility. The unique aspect of the hypersonic nozzle design is the high Mach number entrance conditions, which, for axisymmetric flow, lead to formation of compression waves at the point where the nozzle contour curvature is zero; i.e. when it stops curving away from the axis. This requires that the nozzle be designed to achieve conical source flow using a hyperbolic or horn-shaped profile. Modern CFD can be used in support of test programs to correct conical flow results to uniform flow. A second complicating feature of the nozzle design is the thick incoming tube-wall boundary layer. Also, since boundary layer growth can be quite rapid in hypersonic nozzles, the conventional method-of-characteristics plus displacement thickness correction procedure may be inadequate in accommodating the large viscous effects and further points toward the current design approach. To overcome the inflow nonuniformity, the initial design used a skimmer nozzle to capture only the central more uniform core flow. However, computations showed a larger core flow is obtained by capturing and processing the entire tube exit flow. The specific design operating point for the nozzle is at total enthalpy of 21 MJ/kg; however, the generic hyperbolic nozzle contour should yield nearly conical flow over the entire facility range, from 8-30 MJ/kg, in expansion tunnel mode. This is supported by the final computations for 22.6 and 11.5 MJ/kg which compared well with experiments.

Acknowledgements. We gratefully acknowledge the support of Boeing Reusable Space Systems (Contract # MOM3DXL-454103E). Thanks are also due to NASA Langley Research Center for supporting the calibration of the 12 MJ/kg condition (Contract # NAS1-97027).

References

Adam PH (1997) Enthalpy Effects on Hypervelocity Boundary Layers. Ph.D. thesis. GALCIT, CALTECH, Pasadena, California, USA

Bakos RJ, Calleja JF, Erdos JI, Auslender AH, Sussman MA, Wilson GJ (1996a) Design, Calibration, and Analysis of a Tunnel Mode of Operation for the HYPULSE Facility. AIAA Paper 96-2194

Bakos RJ, Calleja JF, Erdos JI, Sussman MA, Wilson GJ (1996b) An Experimental and Computational Study Leading to New Test Capabilities for the HYPULSE Facility with a Detonation Driver. AIAA Paper 96-2193

Callis LB (1966) An Analysis of Supersonic Flow Phenomena in Conical Nozzles by a Method of Characteristics. NASA TN D-3550

Chue RSM, Tsai C-Y, Bakos RJ, Erdos JI, Rogers RC (2002) NASA's HYPULSE Facility at GASL – A Dual Mode, Dual Driver Reflected-Shock/Expansion Tunnel. In: Lu F, Marren D (eds), Advanced Hypersonic Test Facilities, Progress in Astronautics and Aeronautics, Vol. 198, AIAA, Chapter 3, pp 29–71

Darwell HM, Badham H (1963) Shock Formation in Conical Nozzles. AIAA J. 1(8):1932–1934

Foelsche RO, Rogers RC, Tsai C-Y, Bakos RJ, Shih AT (2001) Hypervelocity Capability of the HYPULSE Shock-Expansion Tunnel for Scramjet Testing. In: Lu F (ed), Proc. 23rd Int. on Shock Waves, Fort Worth, Texas, July 22-27

Jacobs PA (2000) IMOC:Interactive Method of Characteristics for Two-Dimensional Supersonic Flow. Report 3/00 Dept. of Mech. Eng., The Univ. of Queensland, Australia

McGrory WD, Walters RW, Applebaum MP, Eppard WM, Neel R (1996) The General Aerodynamics Simulation Program Version 3, User's Manual. Aerosoft, Inc. Further details of the code can also be obtained from Aerosoft's website at www.aerosft.com

Migdal D, Kosson R (1965) Shock Predictions in Conical Nozzles. AIAA J. 3(8):1554–1556

Migdal D, Landis F (1962) Characteristics of Conical Supersonic Nozzles. ARS J. 32(12):1898–1901

Miller CG (1976) Operational Experience in the Langley Expansion Tube with Various Test Gases and Preliminary Results in the Expansion Tunnel. Presented at the AIAA 9th Aerodynamic Testing Conference, Arlington, Texas, June 7–9

Park C (1993) Review of Chemical-Kinetic Problems of Future NASA Missions, I: Earth Entries. J. Thermophysics Heat Transfer, **7**(3):385–398

Rogers RC, Shih AT, Tsai C-Y, Foelsche RO (2001) Scramjet Tests in a Shock Tunnel at Flight Mach 7, 10, and 15 conditions. AIAA Paper 2001-3241